

Masses and Radii of Spheroidal Magnetized Strange Stars

Samantha López Pérez^{a1}, Daryel Manreza Paret², Gretel Quintero Angulo², Aurora Pérez Martínez¹, and Diana Alvear Terrero¹

¹Departamento de Física Teórica, Facultad de Física, Universidad de la Habana, San Lázaro y L, Vedado, La Habana 10400, Cuba

²Departamento de Física Teórica, Instituto de Cibernética, Matemática y Física, Calle E esq. 15 No. 309, La Habana, CP 10400, Cuba

In this work we study stable configurations of magnetized strange stars using an axially symmetric metric in spherical coordinates and calculate its observables (masses, radii and mass quadrupole moment) [1].

Strange Stars (SSs) are hypothetical stars formed by strange quark matter (SQM), which is speculated to be the true ground state of strongly interacting matter (Bodmer-Witten's conjecture) [4, 5]. This type of stars describe compact objects (COs) with maximum masses around $1.5 M_{\odot}$ and radius of 4–8 km that could account for some observations of cold, dense, and small compact objects that do not fit the standard neutron stars (NSs) models [2]. There are many microscopic models proposed for SSs, all of which differ by how the strong interaction is described and what sort of SQM phases are considered within the star. It's usually describe trough phenomenological models that mimic the main features of Quantum Chromodynamics (QCD) [6]. In particular, we used the MIT Bag model where quarks are considered as quasifree particles confined into a “bag” and having fixed masses [7]. This model reproduces confinement and asymptotic freedom with the use of only one external parameter, the bag energy B_{Bag} .

A well known feature of COs are their extreme superficial and inner magnetic fields, which are estimated to be as high as 5×10^{18} G in the case of NSs. In this case, the energy-momentum tensor of matter is anisotropic and leads to nonspherical stars [9]. We derived and used a set of TOV-like structure equations from an axially symmetric metric in spherical coordinates, the γ equations [9], that allow us to describe spheroidal objects as long as their shape is nearly spherical.

In this work we present a review of previous studies where we study the magnetic field effects on the stability of the SQM and the spheroidal stellar configurations, as well as its observables: mass, radii and the mass quadrupole moment. In addition we compare them with those of spherical strange stars and candidates to be and calculate other observables (eccentricity, moment of inertia and gravitational redshift) that can be found in [1, 3].

Equation of State of Magnetized Strange Stars

We consider SSs composed of SQM and electrons under the action of a uniform and constant magnetic field oriented in the z direction, $B = (0, 0, \mathbf{B})$. As pointed out before, we use the phenomenological MIT bag model

[7] and in this case, we fix the quark masses and charges to $m_u = 2.16$ MeV, $m_d = 4.67$ MeV, $m_s = 93$ MeV, $m_e = 0.51$ MeV, $e_u = \frac{2}{3}e$, and $e_s = e_d = -\frac{1}{3}e$ [8]. After performing an analysis of the stability of magnetized SQM [1], we will use two fixed values of the B_{Bag} constant, 45 MeV/fm³ and 75 MeV/fm³[1].

For a magnetized gas of quarks and electrons, the equations of state are obtained from the thermodynamical potential [6] and the stellar equilibrium conditions

$$\Omega_f(B, \mu, T) = -\frac{e_f d_f B}{\beta} \times \int_{-\infty}^{\infty} \frac{dp_3}{4\pi^2} \sum_{l=0}^{\infty} g_l \sum_{\mathbf{p}_4} \ln[(p_4 + i\mu)^2 + \varepsilon_{lf}^2],$$

where $f = e, u, d, s$ and

$$\varepsilon_{lf}^2 = \sqrt{p_3^2 + 2|e_f B|l + m_f^2},$$

characterizes the spectrum of a charged fermion in a magnetic field. We have designated the Landau levels with l , d_f is the flavor degenerative factor $d_e = 1$, $d_{u,d,s} = 3$ and $g_l = 2 - \delta_{l0}$ takes into account the spin degeneracy of fermions for $l \neq 0$. In addition, μ_f , e_f and m_f are the chemical potential, charge and mass of each particle, respectively. The EoS for the magnetized Strange Star formed by a gas of u , d , s quarks and electrons, taking into account the MIT Bag model, take the form

$$\begin{aligned} E(B, \mu, 0) &= \sum_{\mathbf{f}} [\Omega_f(B, \mu, 0) + \mu_f N_f(B, \mu, 0)] + \\ &\quad + B_{\text{bag}} + B^2/8\pi, \\ P_{\parallel}(B, \mu, 0) &= -\sum_{\mathbf{f}} \Omega_f(B, \mu, 0) - B_{\text{bag}} - B^2/8\pi, \\ P_{\perp}(B, \mu, 0) &= -\sum_{\mathbf{f}} [\Omega_f(B, \mu, 0) + B M_f(B, \mu, 0)] - \\ &\quad - B_{\text{bag}} + B^2/8\pi. \end{aligned}$$

At higher values of the magnetic field, the difference between the perpendicular and parallel pressures is more appreciable. These effects on the EoS will be reflected in the macroscopic structure of the star, as we will see in the next section.

Masses and radii

The axial symmetry imposed in the star by the magnetic field is irreconcilable with the spherical symmetry of standard Tolman-Oppenheimer-Volkoff (TOV) equations. Consequently, it is desirable to use of axisymmetric metrics if one wishes to describe the structure of magnetized COs (see Ref. [9] and references therein). Here, we follow and use a set of axisymmetric structure equations derived from the so-called γ metric [9], where $\gamma = z/r$ accounts for the deformation of the matter source with respect to the spherical shape and parametrizes the polar radius z in terms of the equatorial radius r .

$$ds^2 = - \left[1 - \frac{2Gm(r)}{r} \right]^\gamma dt^2 + \left[1 - \frac{2Gm(r)}{r} \right]^{-\gamma} dr^2 + r^2 \sin^2 \theta d\phi^2 + r^2 d\theta^2,$$

Starting from this metric and considering the anisotropic energy-momentum tensor of magnetized matter, the structure equations (1) are obtained [9]. This system of equations describe the variation of the mass and the pressures with the spatial coordinate r for an anisotropic axially symmetric CO as long as the parameter γ is close to one (See [9] and references therein).

$$\begin{aligned} \frac{dM}{dr} &= 4\pi r^2 \frac{(E_{\parallel} + E_{\perp})}{2} \gamma & (1) \\ \frac{dP_{\parallel}}{dz} &= \frac{1}{\gamma} \frac{dP_{\parallel}}{dr} \\ &= - \frac{(E_{\parallel} + P_{\parallel}) \left[\frac{r}{2} + 4\pi r^3 P_{\parallel} - \frac{r}{2} \left(1 - \frac{2M}{r} \right)^\gamma \right]}{\gamma r^2 \left(1 - \frac{2M}{r} \right)^\gamma} \\ \frac{dP_{\perp}}{dr} &= - \frac{(E_{\perp} + P_{\perp}) \left[\frac{r}{2} + 4\pi r^3 P_{\perp} - \frac{r}{2} \left(1 - \frac{2M}{r} \right)^\gamma \right]}{r^2 \left(1 - \frac{2M}{r} \right)^\gamma}. \end{aligned}$$

In Ref. [9] we proposed the ansatz $\gamma = P_{\parallel c}/P_{\perp c}$, which connects the geometry of the system with the anisotropy produced by the magnetic field. More details about the ansatz and the resolution of γ -equations can be found in [9].

In Figure 1 we show the solutions of γ -equations for several values of the magnetic field. They are compared with the non-magnetized case and with the TOV solutions considering the pairs (E, P_{\parallel}) and (E, P_{\perp}) as independent EoS. In the case of TOV solutions, using one EoS or the other leads to different mass-radius relations, whose differences increase with the magnetic field. For a given energy density range, a higher pressure implies bigger and massive stars. Also, for a fixed value of the magnetic field, the difference in the stars size obtained with the pairs (E, P_{\parallel}) and (E, P_{\perp}) , is larger for heavier stars. This suggest that more massive stars will have a greater deformation. Unlike TOV equations, γ -equations allow us to model the star as a spheroidal with an equatorial radius R and a polar ra-

dius Z . So, in Figure 1 the $M-R$ and $M-Z$ curves correspond to a unique sequence of stars, while the $M-R_{\perp}$ and the $M-R_{\parallel}$ curves stand for two different sequences with (E, P_{\perp}) and EoS (E, P_{\parallel}) , respectively. The low and median bands correspond to objects PSR J1614-2230 and PSR J0348 + 0432 with $M = 1.97 \pm 0.04 M_{\odot}$ [10] and $M = 2.01 \pm 0.04 M_{\odot}$ [11]. The upper band represents the new result of $2.14^{+0.10}_{-0.09} M_{\odot}$ for the mass of the pulsar MSP J0740+6620 to a confidence interval of 68.3% presented in [12]. The range of allowable parameters is further constrained by recent mass-radius estimates extracted from NICER data, $M = 1.44^{+0.15}_{-0.14} M_{\odot}$ with $R = 13.02^{+1.24}_{-1.06}$ km [13], $M = 1.34^{+0.15}_{-0.16} M_{\odot}$ with $R = 12.71^{+1.14}_{-1.19}$ km [14] and $R_{1.44} > 10.7$ km [15]. These estimates are indicated by the black dots with their corresponding error bars.

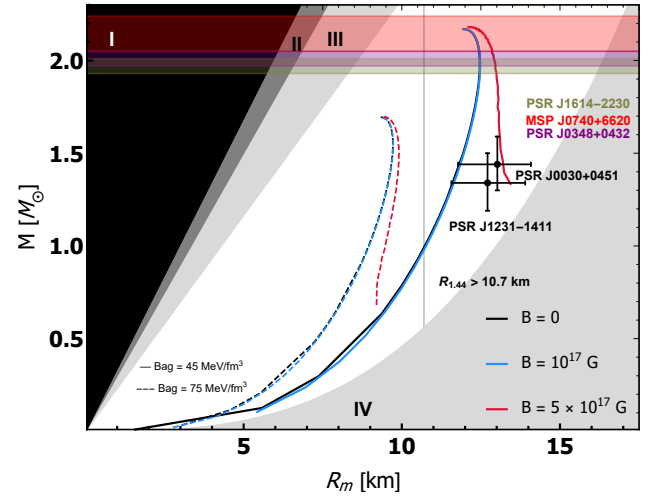


Figure 1: Solutions for spheroidal configurations in comparison with the non-magnetized configuration at $B = 10^{17}$ G and $B = 5 \times 10^{17}$ G, where R_m represents the mean radius defined such that the sphere it determines is equal to the surface area of the spheroidal star $A = 2\pi R [R + \frac{Z}{\varepsilon} \arcsin \varepsilon]$. Gravitational stability requirement (I). Finite pressure requirement (II). Causality requirement (III). Rotational stability requirement (IV).

The stellar configurations obtained are oblate objects ($R > Z$), as expected since $P_{\perp} > P_{\parallel}$ [1]. On the contrary of what happens with TOV solutions, for which the difference between R_{\perp} and R_{\parallel} increases with the mass, the deformation of our spheroidal stars—the differences between the equatorial and the polar radius—decreases with the mass. Hence, the importance of building a model, as the one we present, that takes into account both pressures simultaneously.

Mass quadrupole moment

The quadrupole moment due to the magnetic field is directly related to the amplitude of the OGS [1], since they are only emitted in situations where a mass asymmetry is generated that gives rise to a quadrupole moment, either as a consequence of rota-

tion or the magnetic field. Therefore, spherical stars do not have a quadrupole momentum and cannot generate OGs. In contrast, magnetized stars, being deformed, have non-zero quadrupole moments that can contribute to the emission of GWs. In the framework of our structure equations, the quadrupole moment of the SSs is $Q = \frac{2}{3}M^3(1 - \gamma^2)$ (See [9] and references therein), where $\gamma = 1$ implies $Q = 0$, which corresponds to the spherical case. Figure 2 shows this magnitude as a function of the star's mass. The oscillations in the curves are an effect of the presence of the sum by the Landau levels in the EoS. Q diminishes with B_{Bag} and its maximum is reached for stars in the region of intermediate mass and deformation. This behavior is due to the simultaneous dependence of Q on M and γ , which in particular is determined by the fact that γ depends on the EoS and thus therefore varies between stars. This result is different from the one obtained in Ref. [16], where equations of structure derived from the γ metric were solved by taking γ as a free parameter. In this case the highest values of the quadrupole are reached for the most massive stars. Therefore, connecting γ to the physics of the problem has a direct impact on the observables, and can serve as a way to discriminate between models.

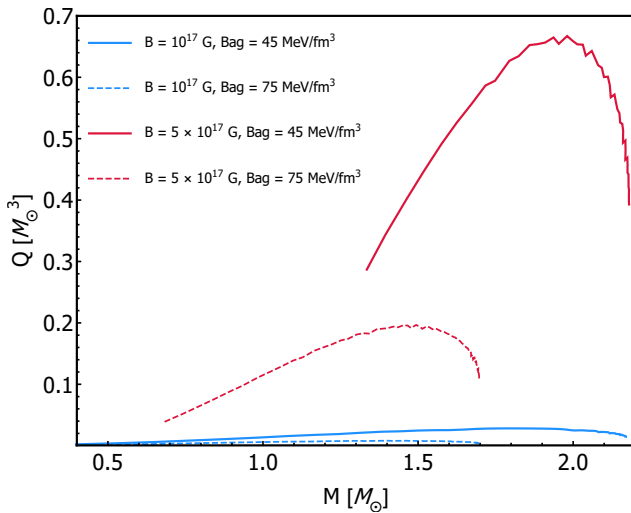


Figure 2: Mass quadrupole moment Q as a function of mass M at $B = 10^{17}$ G, $B = 5 \times 10^{17}$ G for $B_{\text{bag}} = 45$ MeV/fm³ and $B_{\text{bag}} = 75$ MeV/fm³ [1].

Conclusions

In our model, less massive stars suffer bigger deformations in contrast with the results from TOV solutions for the perpendicular and the parallel pressure independently. The stable stellar sequences obtained are in the region allowed by the theoretical constraints for mass and radius values, and are close to the observational values for masses and radii of different pulsars. This supports the physical plausibility of our model of magnetized strange stars. Since the magnetized SS is deformed, it has a quadrupole momentum, the value of

which is maximum in the intermediate regions of mass and radius, so stars in these regions are expected to produce the most intense GWs. The mass quadrupole moment depends explicitly on the deformation through the EoS because γ appears on their mathematical expression. This reveals the model dependency of the results and highlights how important is the construction of even more realistic models.

Notes

a. Email: samantha@icimaf.cu

References

- [1] D. Alvear Terrero, S. López Pérez, D. Manreza Paret, A. Pérez Martínez, G. Quintero Angulo. *Phys. Rev. C* **103** (2021) 045807
- [2] T. Gangopadhyay, S. Ray, X.-D. Li, J. Dey, M. Dey. *Mon. Not. Roy. Astron. Soc.* **431** (2013) 3216–3221
- [3] S. L. Pérez, D. Manreza-Paret, G. Q. Angulo, A. Pérez Martínez, D. Alvear Terrero. *Astron. Nachr.* **342**, no. 1-2 (2021) 326–331
- [4] A. R. Bodmer. *Phys. Rev. D* **4** (1971) 1601–1606
- [5] E. Witten. *Phys. Rev. D* **30** (1984) 272–285
- [6] D. Manreza Paret, J. E. Horvath, A. Pérez Martínez. *Research in Astronomy and Astrophysics* **15** (2015) 975
- [7] A. Chodos, R. L. Jaffe, K. Johnson, C. B. Thorn and V. F. Weisskopf *Phys. Rev. D* **9** (1974) 3471–3495
- [8] Particle Data Group and Zyla, P. A. and Barnett, R. M., Beringer, J. et al. *Progress of Theoretical and Experimental Physics* **9** (2020) 2050-3911
- [9] D. Alvear Terrero, V. Hernández Mederos, S. López Pérez, D. Manreza Paret, A. Pérez Martínez, G. Quintero Angulo. *Phys. Rev. D* **99** (2019) 023011
- [10] P. B. Demorest, T. Pennucci, S. M. Ransom, M. S. E. Roberts, J. W. T. Hessels. A two- solar-mass neutron star measured using Shapiro delay. *Nature* **467** (2010) 1081–1083
- [11] J. Antoniadis et al. A Massive Pulsar in a Compact Relativistic Binary. *Science* **340** (2013) 6131
- [12] H. T. Cromartie et al. Relativistic Shapiro delay measurements of an extremely massive millisecond pulsar. *Nature Astron.* **4** (2019) 72–76
- [13] M. C. Miller et al. PSR J0030+0451 Mass and Radius from NICER Data and Implications for the Properties of Neutron Star Matter. *Astrophys. J. Lett.* **887** (2019) L24

- [14] T. E. Riley et al. A NICER View of PSR J0030+0451: Millisecond Pulsar Parameter Estimation. *Astrophys. J. Lett.* **887** (2019) L21
- [15] S. Bogdanov et al. Constraining the Neutron Star Mass-Radius Relation and Dense Matter Equation of State with NICER. III. Model Description and Verification of Parameter Estimation Codes. *Astrophys. J. Lett.* **914** (2021) L15
- [16] O. Zubairi, A. Romero, F. Weber. CStatic solutions of Einstein's field equations for compact stellar objects. *J. Phys. Conf. Ser.* **615** (2015) 012003